

MODELLING AND IDENTIFICATION OF THE MECHANICAL BEHAVIOUR OF OXIDE/OXIDE CERAMIC MATRIX COMPOSITES

C. Ben Ramdane^{1*}, A. Jankowiak², J.-F. Maire², M. Parlier², P. Diss¹, E. Martin³

¹Herakles (Safran Group), Department of Materials Development, Les 5 Chemins 33187 Le Haillan, France

²Onera, Department of Composite Materials and Structures, 29 Avenue de la Division Leclerc 92322 Châtillon, France

³Laboratoire des Composites Thermostructuraux, 3 Allée de la Boétie 33600 Pessac, France

*camelia.ben_ramdane@onera.fr

Keywords: CMCs, oxide, weak matrix, damage mechanics.

Abstract

Porous-matrix oxide/oxide composites are candidate materials for thermostructural applications. Hence, it is necessary to be able to predict their mechanical behaviour through a continuum damage model. In order to establish such a model, it is required to run several experimental tests on the material of interest, a Nextel™ 610/alumina composite. The first experimental results are presented. It is shown that, under tensile loading in the fiber direction, the studied composite is almost linear to failure. Finally, the different equations of the model that is most certainly going to be used are also presented.

1 Introduction

Regarding the current environmental context, decreasing the greenhouse effect of gases exhausted by turbojet engines is an urgent necessity. Therefore, aircraft manufacturers are developing improved turbojet engines which exhaust systems require thermostable materials up to 1000°C. Due to their good thermo-mechanical properties, ceramic matrix composites (CMCs) are candidate materials for such applications at high temperature. However, non-oxide CMCs materials are subjected to severe deteriorations under typical operating conditions in turbojet engines. Experimental results showed that oxide fibre/non-oxide matrix or non-oxide fibre/oxide matrix composites were not resistant to oxidation [1]. All-oxide CMCs have been studied for a few years because of their better oxidation resistance. Moreover, their fabrication processes are cheaper than those of other CMCs that are elaborated by chemical vapour infiltration (CVI).

The present research is focused on an alumina/alumina composite with a 2D woven fibre reinforcement and a weak porous matrix. Actually, the porosity enables the crack deflection in the matrix, avoiding fibre damage without the necessity of a fibre coating. The present work is aimed at understanding the mechanical behaviour of such composites in order to establish and identify a constitutive law.

2 Material design

Two different approaches have been developed in order to avoid brittle fracture in continuous fibre ceramic matrix composites. The first one is based on the very weak fibre/matrix interface bonding. In this approach, a fibre coating is required. The coating introduces weak

interfaces that deflect cracks at the fibre/coating and/or coating/matrix interfaces and enables a subsequent fibre debonding. The second approach is based on a weak porous matrix. Indeed, the matrix micro- and macropores promote crack deflection at the fibre/matrix interface, leading to fibre debonding and pull-out, thereby increasing the composite toughness and avoiding brittle fracture behaviour [2-7]. In this approach, it is mandatory to control the pore size and the fine distribution of the porosity within the matrix [3,8]. The microstructure must be designed such that the matrix is sufficiently weak to promote crack deflection and strong enough to maintain the off-axis and interlaminar strength of the composite.

Weak matrix composites have a different mechanical behaviour compared to weak interface composites. The weak matrix approach takes into account the fact that a strong interface exists between the fibres and the matrix. In this case, because of the low elastic stiffness and fracture toughness of the matrix (due to porosity), cracks do not readily propagate from the matrix to the fibres and tensile loading leads to extensive damage in the matrix before failure of the fibres [7]. In order to prevent strong matrix/fibre interactions under manufacturing or operating conditions, the choice of the matrix/fibre couple is essential [2].

The studied composite is a Nextel™ 610/alumina oxide/oxide CMC manufactured at Onera consisting of a porous alumina matrix reinforced with 2D Nextel™ 610 fabric with no fibre coating. The damage tolerance of such a CMC is enabled by the porous matrix.

3 Experimental procedure

3.1 Manufacturing process

The Nextel™ 610 8 harness satin weave (8HSW) fabric reinforcement was supplied by 3M Company. This fabric is orthotropic and can be considered as symmetric. The Nextel™ 610 fibres are fully crystalline and contain more than 99 wt% of pure α -alumina with a grain size of approximately 0.1 μm [2]. These fibres are free of glassy phases and, thus, are very chemically stable even in corrosive atmospheres. Moreover, due to their ultra-fine grain size, the Nextel™ 610 fibres have a high creep resistance up to 1000°C [2]. However, because the fibres are single-phased, their strength rapidly decreases for temperatures higher than 1000°C due to grain growth. The average fibre diameter is $11.52 \pm 0.22 \mu\text{m}$. A Nextel™ 610 single filament has an average tensile strength of 3.3 GPa, a tensile modulus of 373 GPa, a density of 3.9 $\text{g}\cdot\text{cm}^{-3}$ and a maximum use temperature of 1000°C (at 1% strain and 69 MPa during 1000 hours) [10].

The matrix is an α -alumina powder with a bulk density of 0.8 $\text{g}\cdot\text{cm}^{-3}$ and a submicronic particle size. A slurry of this powder is prepared in de-ionised water with 1wt% of an organic binder.

The manufacturing process of the Nextel™ 610/alumina composites can be divided into four steps. The first step is the impregnation of desized fibre fabric with matrix slurry. Then, the fibre fabrics are cut into plies that are laid up and hot moulded in a press under vacuum. The last step is a heat treatment for matrix sintering.

The composite plates are made out of 12 woven 2D fabric layers and are approximately 2.3 mm thick, with a fibre volume fraction of approximately 50% and a porosity of approximately 25% [11].

3.2 Composite microstructure

The microstructure must be designed to have a sufficiently low toughness to enable crack deflection through the matrix while maintaining enough strength for adequate off-axis and interlaminar properties [9]. The fine grained alumina matrix used in this study allows a good infiltration of the matrix between the fibre fabric layers and within the fibre tows. The heat treatment involves matrix shrinkage which generates matrix cracks perpendicular to fabric layers. SEM micrographs (figure 1) illustrate the composite microstructure.

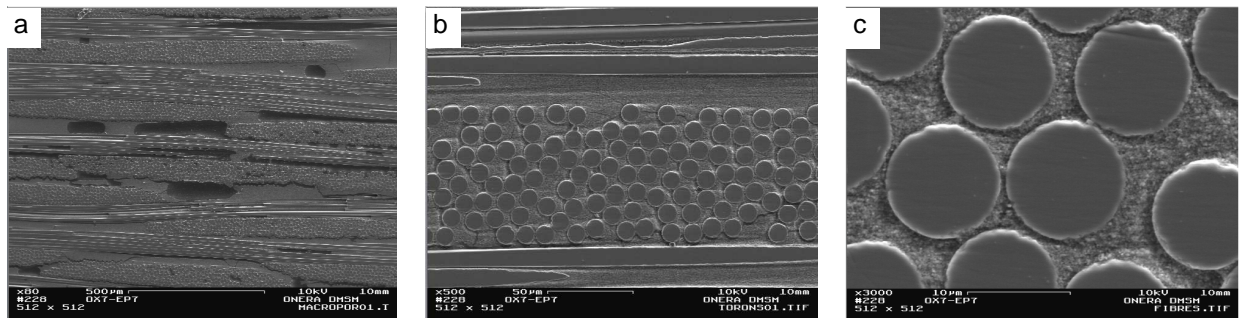


Figure 1. SEM transverse cross section micrographs showing the microstructure of Nextel™ 610/alumina composites. a. General view of the material, showing the fibre fabric layers, the macropores and matrix cracks within as-processed composites. b. Infiltration of the matrix in the fibre tows and between the plies. c. Higher magnification of a fibre tow showing the good infiltration of the fine-grained matrix into the tow.

Because of the development of matrix cracking, these materials exhibit a non-linear mechanical behaviour [12].

3.3 Test procedures

In order to establish a model describing the mechanical behaviour of the studied composite material, several mechanical tests are required. The monotonic tension tests in the directions of the fibres and with a $\pm 45^\circ$ fibre direction can be used to emphasize the behaviour of the fibre tows and matrix. If the fibres are 0° or 90° oriented to the loading axis, then the mechanical behaviour of the composite is dominated by the fibres, while it is matrix-dominated with a $\pm 45^\circ$ fibre orientation. Incremental cyclic tension-compression tests give the residual strain of the composites and permit to assess the incidence of damage evolution (from modulus changes) as well as the occurrence of internal friction (from hysteresis strains) [9,12]. The compression solicitation following the return to zero stress enables the closure of the matrix cracks induced by the previous tension solicitation. Thus, the material recovers its initial elastic properties. Flexure tests will also be necessary to identify the interlaminar shear strength of the composite.

The testing machine used was an Adamel Lhomargy DY 26 under displacement control using a displacement rate of $0.5 \text{ mm}\cdot\text{min}^{-1}$. Longitudinal deformation was measured with the help of digital image correlation (DIC) and an extensometer. In order to avoid the damage of the sample at the grip jaws and the damage of the samples by the grip jaws, annealed aluminium tabs were placed between the end side of the sample and the grip jaw. All the tests mentioned thereafter were run at room temperature.

Tension tests run on samples of different widths showed that this parameter had little influence on the sample strength. However, the fracture surfaces were different from a width to another (figure 2). All samples show a marked fibre pull-out but this phenomenon is more pronounced on the widest ones, which are particularly brushy. Then, all the straight sided samples used for tension tests were 16 mm wide, 150 mm long and approximately 2.3 mm thick.

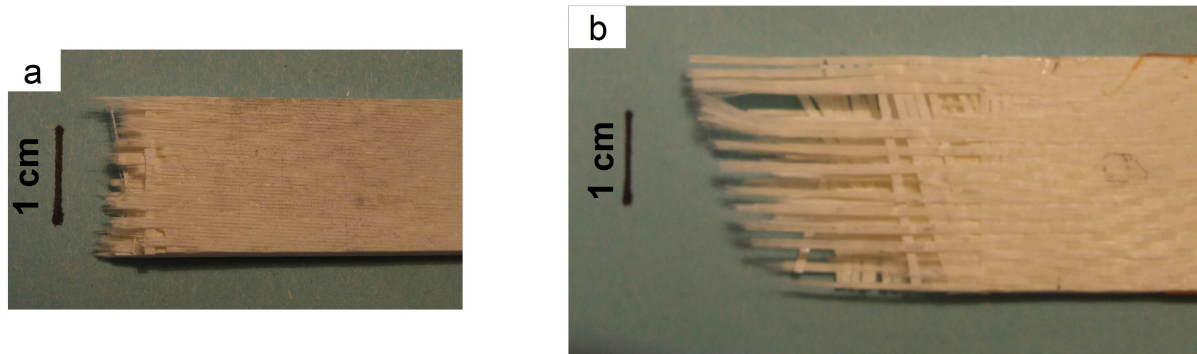


Figure 2. Fracture surface of monotonic tension samples of: a. 16 mm width and b. 25 mm width.

4 Results and discussion

4.1 Mechanical properties under tensile loading

The stress-strain curves obtained for the 0° fibre direction are nearly linear to failure (figure 3). Material exhibits typical fibre-dominated composite behaviour. On each curve, two linear parts can be distinguished, the first one corresponding to the elastic domain.

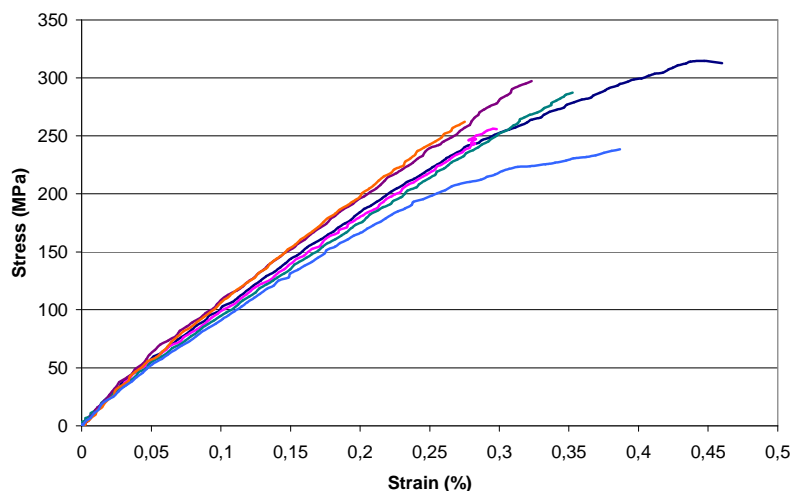


Figure 3. Tensile stress-strain curves for 6 Nextel™ 610/alumina ceramic composite samples at room temperature. The samples were cut from different plates.

The average ultimate tensile strength (UTS) is 276 ± 28 MPa, the average elastic modulus is 120 ± 8 GPa and the average failure strain is 0.35 ± 0.07 %. The dispersion of the data is quite large, but this is generally the case with CMCs. As already mentioned, the Nextel™ 610 8HSW fabric is orthotropic and can be considered as symmetric. Thus, the tensile behaviour in the 90° fibre direction is expected to be the same as in the 0° fibre direction.

Only a few data about the damage mechanisms of oxide/oxide composites is available in published research articles. SEM micrographs of cross sections of tensile samples illustrate the crack patterns in the composite (figure 4.a, 4.b and 4.c). According to these micrographs, it can be assumed that, first, under tensile loading, the cracks propagate along the longitudinal fibre tows (figure 4.a). This phenomenon may have two origins. Firstly, cracks initiated on pores in the porous matrix may be deflected at the fibre/matrix interfaces along the fibre tows. Secondly, the straightening of the woven longitudinal tows under the effect of the tensile

loading may induce a complex stress system in the fibre tows and in the matrix, thus leading to fibre/matrix debonding. Such a mechanism leads to both intraply and interply debonding (figure 4.b). Cracks also propagate within the longitudinal tows (figure 4.c). Finally, when the load increases and reaches the ultimate tensile stress, the composite fails and fibre pull-out is observed on the fracture surface (figure 4.d).

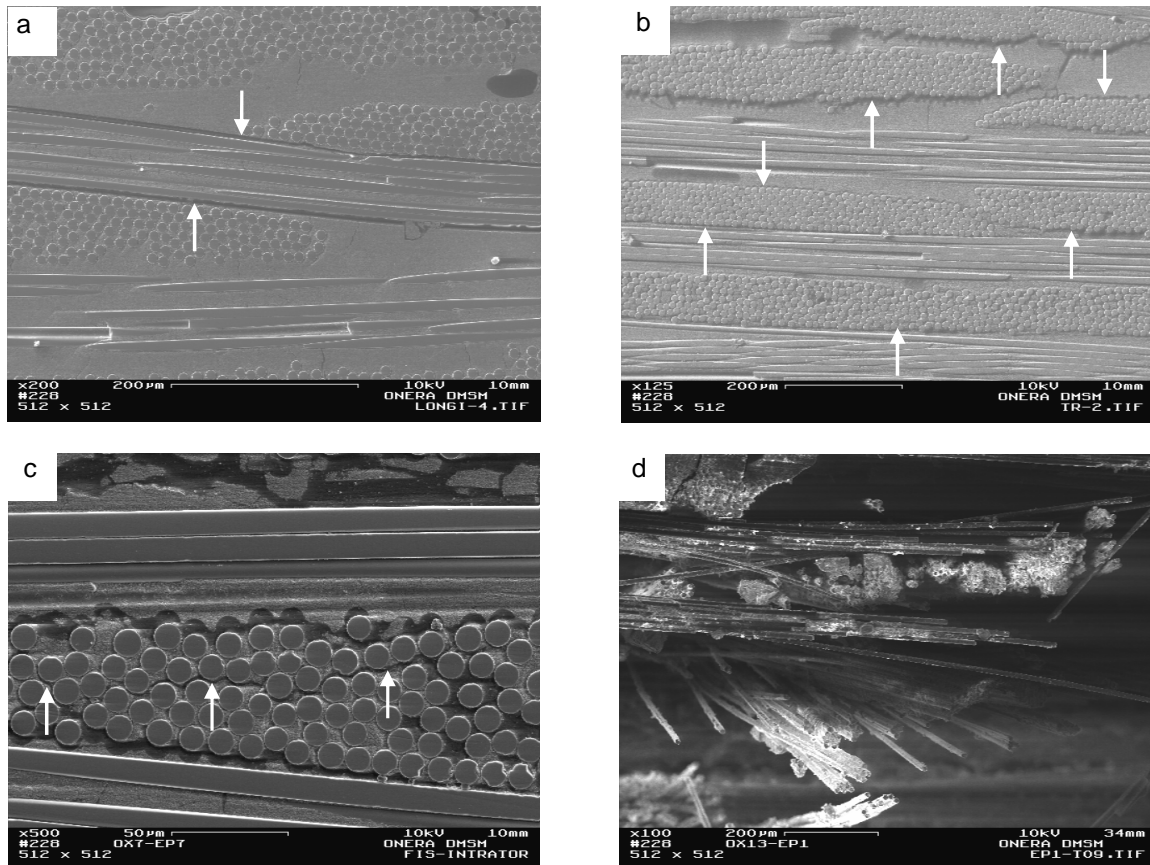


Figure 4. Microstructural views of Nextel™ 610/alumina composites after tensile test in the fibre direction.
 a. Propagation of a matrix crack at the periphery of a longitudinal tow (longitudinal cross-section).
 b. Propagation of matrix cracks at the periphery of the longitudinal tows (transverse cross-section).
 c. Propagation of cracks in a longitudinal tow (transverse cross-section). d. Fibre pull-out after failure.

4.2 Modelling

In order to predict the mechanical behaviour of structures, it is necessary to establish a continuum damage mechanics model describing the non-linear response of the composite. Hence, the model must take into account the matrix and fibre damage phenomena, from the elastic response till progressive failure of fibre bundles and ruin of the material. The model that will be used to describe the mechanical behaviour of oxide/oxide composites is the Onera Damage Model (ODM) [13,14], developed over the past several years at Onera. This model is thermodynamically admissible.

Because of the important difference between matrix and fibres mechanical properties, the mechanical behaviour of porous matrix oxide/oxide composites is very anisotropic. Thus, the damage orientation depends on the microstructure. Hence the effect of matrix damage is described by three damage variables, one for the 0° fibre direction (d_1^m), one for the 90° fibre direction (d_2^m) and the last one for the out-of-plane direction (d_3^m). Because of the

assumption of symmetry for the studied orthotropic fabric, the evolution of the damage variables d_1^m and d_2^m are equal.

The propagation of microcracks induces a progressive decrease in the elastic properties during tensile loading, whereas, under compression loading, closure of the microcracks leads partially to the recovery of the initial elastic properties [15]. These variations will be taken into account in the damage effect tensors \underline{H}_i^m and by the activation indexes η_i^m . We distinguish two damage effects tensors: \underline{H}_i^{m+} for open microcracks and \underline{H}_i^{m-} for closed microcracks. The η_i^m indexes are used to describe the state of the matrix cracks, that can be opened, closed (under compression loading) or in an intermediate state. ODM takes into account the fact that, even if the matrix cracks are closed, the damage can still exist. The same variables and tensors are defined for the fibre bundles, with a distinction between tension and compression. Hence, the effective compliance tensor of the material can be defined as:

$$\underline{S}^{eff} = \underline{S}^0 + \Delta\underline{S}^m + \Delta\underline{S}^f \quad (1)$$

where \underline{S}^0 is the initial compliance tensor of the composite material, $\Delta\underline{S}^m$ is the compliance tensor of the effect of matrix damage and $\Delta\underline{S}^f$ is the compliance tensor of the effect of fibre damage. These tensors are defined as follows:

$$\Delta\underline{S}^m = \sum_{i=1}^3 d_i^m (\eta_i^m \underline{H}_i^{m+} + (1-\eta_i^m) \underline{H}_i^{m-}) \quad (2)$$

$$\Delta\underline{S}^f = \sum_{i=1}^3 d_{it}^f (\eta_{it}^f \underline{H}_{it}^{f+} + (1-\eta_{it}^f) \underline{H}_{it}^{f-}) + \sum_{i=1}^3 d_{ic}^f (\eta_{ic}^f \underline{H}_{ic}^{f+} + (1-\eta_{ic}^f) \underline{H}_{ic}^{f-}) \quad (3)$$

Finally, the mechanical behaviour of porous matrix oxide/oxide composites can be described by:

$$\underline{\sigma} = \underline{C}^{eff} : (\underline{\varepsilon} - \underline{\varepsilon}^{th} - \underline{\varepsilon}^0) - \underline{C}^f : (\underline{\varepsilon}^r + \underline{\varepsilon}^s - \underline{\varepsilon}^0) \quad (4)$$

with:

$$\underline{C}^{eff} = (\underline{S}^{eff})^{-1} = (\underline{S}^0 + \Delta\underline{S}^m + \Delta\underline{S}^f)^{-1} \quad (5)$$

$$\underline{C}^f = (\underline{S}^f)^{-1} = (\underline{S}^0 + \Delta\underline{S}^f)^{-1} \quad (6)$$

where:

$\underline{\sigma}$ is the stress tensor;

\underline{C}^{eff} is the effective stiffness tensor;

\underline{C}^f is the stiffness tensor of the fibres;

$\underline{\varepsilon}$ is the strain tensor;

$\underline{\varepsilon}^0$ is the strain tensor corresponding to closed microcracks;

$\underline{\varepsilon}^{th}$ is the thermal strain tensor;

$\underline{\varepsilon}^r$ is the residual strain tensor,

$\underline{\varepsilon}^s$ is the stocked strain tensor.

5 Conclusion

The studied material is a Nextel™ 610/alumina with a porous matrix and a 2D woven reinforcement. In order to establish a continuum damage mechanics model able to predict the mechanical behaviour of this oxide/oxide CMC, several experimental tests have to be run. Tension tests showed that, in the fibre direction, the stress-strain curve is almost linear to failure. The composite material still has to undergo tension tests in $\pm 45^\circ$ fibre direction, compression tests and incremental tension-compression tests in 0° and $\pm 45^\circ$ fibre directions. These tests will enable us to determine the parameters of the continuum damage mechanics model (ODM). A few other tests, such as, for example, flexion and interlaminar shear tests, will be performed to fully determine the parameters of the constitutive law. The model will then be included in a finite element code in order to predict the mechanical behaviour of structures made out of Nextel™ 610/alumina composite.

References

- [1] Ruggles-Wrenn M.B., Radzicki A.T., Baek S.S., Keller K.A., Effect of loading rate on the monotonic tensile behavior and tensile strength of an oxide-oxide ceramic composite at 1200°C , *Materials Science and Engineering A*, **492**, pp. 88-94 (2008).
- [2] Wilson D.M., Visser L.R., High performance oxide fibers for metal and ceramic composites, *Composites Part A*, **32**, pp. 1143-1153 (2001).
- [3] Ruggles-Wrenn M.B., Musil S.S., Mall S., Keller K.A., Creep behavior of Nextel™ 610/monazite/alumina composite at elevated temperatures, *Composites Science and Technology*, **66**, pp. 2089-2099 (2006).
- [4] Ruggles-Wrenn M.B., Mall S., Eber C.A., Harlan L.N., Effects of steam environment on high-temperature mechanical behavior of Nextel™720/alumina (N720/A) continuous fiber ceramic composite, *Composites Part A*, **37**, pp. 2029-2040 (2006).
- [5] Haslam J.J., Berroth K.E., Lange F.F., Processing and properties of an all-oxide composite with a porous matrix, *Journal of the European Ceramic Society*, **20**, pp. 607-618 (2000).
- [6] Zok F.W., Levi C.G., Mechanical properties of porous-matrix ceramic composites, *Advanced Engineering Materials*, **3**, pp. 15-23 (2001).
- [7] Davis J.B., Marshall D.B., Morgan P.E.D., Oxide composites of Al_2O_3 and LaPO_4 , *Journal of the European Ceramic Society*, **19**, pp. 2421-2426 (1999).
- [8] Lev L.C., Argon A.S., Oxide-fiber-oxide-matrix composites, *Materials Science and Engineering A*, **195**, pp. 251-261 (1995).
- [9] Levi C.G., Yang J.Y., Dalglish B.J., Zok F.W., Evans A.G., Processing and performance of an all-oxide ceramic composite, *Journal of the American Ceramic Society*, **81**, pp. 2077-2086 (1998).
- [10] Wilson D.M., New High Temperature Oxide Fibers, *publication of the 3M Co., St. Paul, MN, USA*
- [11] Parlier M., Ritti M.-H., Jankowiak A., Potential and Perspectives for Oxide/Oxide Composites, *AerospaceLab*, **3**, paper AL3-09 (2011).
- [12] Marcin L., *Modélisation du comportement, de l'endommagement et de la rupture de matériaux composites à renforts tissés pour le dimensionnement robuste de structures*, PhD. Thesis of the Université de Bordeaux 1 (2010)

[13] Marcin L., Maire J.-F., Carrère N., Martin E., Development of a Macroscopic Damage Model for a Woven Ceramic Matrix Composite, *International Journal of Damage Mechanics*, **20**, pp. 939-957 (2011).

[14] Maire J.-F., Chaboche J.-L., A new formulation of Continuum Damage Mechanics (CDM) for Composite Materials, *Aerospace Science and Technology*, **4**, pp. 247-257 (1997).